https://doi.org/10.5194/egusphere-2025-1381
Preprint. Discussion started: 21 May 2025

Impact of tropical oceans on dipole-like surface mass balance trends in West Antarctica

Kai Man[1,2], Xichen Li[1*], Jürg Luterbacher[3], Lei Geng[4], Naiming Yuan[5,6,7], Yurong Hou[1,2], Yonghao Wang[1,2], Yujie Miao[1,2]

[1]Institute of Atmospheric Physics, Chinese Academy of Sciences, Beijing, China.
[2]University of Chinese Academy of Sciences, Beijing, China.
[3]Center for International Development and Environmental Research and Department of Geography, Justus Liebig University, Giessen, Germany
[4]School of Earth and Space Sciences, University of Science and Technology of China, Hefei, Anhui, China
[5]School of Atmospheric Sciences, Sun Yat-sen University, Zhuhai, China
[6]Key Laboratory of Tropical Atmosphere-Ocean System (Ministry of Education), Zhuhai, China
[7]Southern Marine Science and Engineering Guangdong Laboratory, Zhuhai, China.

Correspondence to: Xichen Li (lixichen@mail.iap.ac.cn)

Abstract. The surface mass balance (SMB) of the Antarctic Ice Sheet is a critical factor in influencing global mean sea level rise and has substantial implications for future projections of sea level rise. In recent decades, the Antarctic Ice Sheet SMB trends show pronounced regional disparities, marked by an increase over the western part but a decrease over the eastern part of West Antarctica. Through a synthesis of ice core records and five reanalysis datasets, as well as atmospheric dynamics analysis and numerical model simulations, we demonstrate that the multi-decadal trends in tropical sea surface temperature are key drivers of the dipole-like SMB trends in West Antarctica. Specifically, the eastern tropical Pacific cooling associated with the phase changes of the Interdecadal Pacific Oscillation (IPO) and the tropical Atlantic warming associated with the Atlantic Multi-decadal Oscillation (AMO) stimulate Rossby wave trains propagating to the West Antarctic, resulting in the contrasting moisture divergence and precipitation changes between the western and eastern parts of West Antarctica. In particular, the statistical analysis and model simulation clarify the seasonality of these teleconnections. Both the Pacific and Atlantic contribute to the dipole-like SMB pattern during austral spring and autumn, while the Pacific is the major contributor during austral summer. Our findings have broad implications for understanding the recent observed SMB trends as well as the projecting future changes in the Antarctic SMB and consequent global sea level rise.

1 Introduction

The mass loss of the Antarctic ice sheet has accelerated over the past four decades due to the enhanced ice discharge across the ice sheet grounding line, largely contributing to the global sea level rise (Fox-Kemper et al., 2021; Rignot et al., 2019; Shepherd et al., 2018). This dynamical mass loss is primarily attributed to the ice shelf basal melting (Pritchard et al., 2012) driven by the sub-surface ocean warm water intrusion (Holland et al., 2020; Thomas et al., 2023). Conversely, the

https://doi.org/10.5194/egusphere-2025-1381
Preprint. Discussion started: 21 May 2025

total surface mass balance (SMB) of the Antarctic ice sheet has increased over the past century (Medley and Thomas, 2019; Wang and Xiao, 2023), offsetting the coastal mass loss. Several processes, including the amount of, sublimation, drifting snow erosion and runoff contribute to the SMB over the Antarctic ice sheet, while precipitation amount plays a dominant role (Agosta et al., 2019; van Wessem et al., 2018).

Recent studies have revealed that multi-decadal trends in the Antarctic SMB show regional disparities (Dalaiden et al., 2022; Lenaerts et al., 2019; Medley et al., 2018; Medley and Thomas, 2019), which hinders the evaluation of its integrated contribution to the mass change of the Antarctic Ice sheet (King and Watson, 2020). Firn and ice core records show significant increases in SMB in the Dronning Maud Land and the Weddell Sea coast in recent decades (Medley et al., 2018), while atmospheric reanalysis data indicate declining annual precipitation trends in the Wilkes Land and the western Ross Ice Shelf (Lenaerts et al., 2019). Remarkably, a dipole-like trend in SMB has been observed over West Antarctica in recent decades, as reconstructed from ice core records, with an increase in the Ellsworth Land and Peninsula and a decrease in the Marie Byrd Land, representing the most pronounced trend pattern across Antarctica (Dalaiden et al., 2022; Medley and Thomas, 2019). Understanding the drivers behind these regional disparities of SMB trends in West Antarctica is crucial for projecting future mass changes in the Antarctica Ice Sheet.

Several mechanisms have been proposed to explain the multi-decadal changes in the West Antarctic SMB. It is found that changes in the atmospheric moisture-holding capacity due to global warming increase annual precipitation amount (Frieler et al., 2015). The sea ice reduction (Wang et al., 2017) around the Antarctic and the sea surface warming over the Southern Ocean (Kittel et al., 2018) enhance moisture transport from the ocean to the ice sheet. At the same time, the changes in the high-latitude Southern Hemisphere atmospheric circulations in recent decades, including a positive trend in the Southern Annular Mode (SAM) (Fogt and Marshall, 2020) related to the ozone depletion (Chemke et al., 2020; Lenaerts et al., 2018), and the intensification of the Amundsen Sea Low (ASL) (Dalaiden et al., 2022; Raphael et al., 2016), have also been identified as significant contributors.

Regional climate changes over the Antarctic have been largely attributed to the drivers from lower latitudes through tropical–polar teleconnections (Ding and Steig, 2013; Li et al., 2021). Recent studies reveal that the interannual variabilities of tropical sea surface temperature (SST), e.g., El Niño–Southern Oscillation (ENSO) and Indian Ocean Dipole (IOD) (Saji et al., 1999), impact the sea ice concentration (Nuncio and Yuan, 2015; Yuan and Martinson, 2001) and surface air temperature (Ding and Steig, 2013) in the Antarctic. Recent studies indicated that tropical-polar teleconnection may also potentially contribute to the SMB changes over the Antarctic continent (Bodart and Bingham, 2019; Donat-Magnin et al., 2020; Ekaykin et al., 2004; Marshall et al., 2017; Thomas et al., 2015; Turner et al., 2019), with the main focus on the remote effect of ENSO events (Bodart and Bingham, 2019; Donat-Magnin et al., 2020; Turner et al., 2019). Beyond interannual variability, tropical SSTs exhibit substantial multi-decadal changes linked to the phases of the Interdecadal Pacific Oscillation (IPO) (Henley et al., 2015; Zhang et al., 1997) and Atlantic Multi-decadal Oscillation (AMO) (Schlesinger and Ramankutty, 1994). Over the past decades, the Atlantic has remained in a positive AMO phase (Yang et al., 2020), while the Pacific experienced a negative phase of IPO after the late 1990s (Jiang and Zhou, 2023). Concurrently, the

https://doi.org/10.5194/egusphere-2025-1381
Preprint. Discussion started: 21 May 2025

Indian Ocean has experienced pronounced warming. These multi-decadal changes in tropical SSTs have been identified as key drivers of atmospheric circulation changes (Li et al., 2021; Clem and Fogt, 2015), ice shelf melting (Jenkins et al., 2018) and sea ice retreat (Meehl et al., 2019). However, their potential contribution to SMB trends over Antarctica during recent decades remains unclear.

In this study, we combine ice core records with reanalysis datasets to investigate both annual and seasonal SMB changes in West Antarctica and their underlying mechanisms. Specifically, we demonstrate that multi-decadal trends in tropical sea surface temperatures contribute to the dipole-like SMB patterns in West Antarctica through atmospheric teleconnections.

2 Data and Methods

2.1 Data

2.1.1 Observational records

Ice cores provide valuable and sparse SMB data, despite limitations such as large local noise (Cavitte et al., 2020) and chronological uncertainties (Bouchet et al., 2023). To extract the large-scale changes over the entire West Antarctic continent, we analyze SMB in 21 ice cores spreading West Antarctica. Given that all the cores were drilled before 2010, the annual SMB data is limited up to that year. In several locations, more than one ice cores were drilled. Before we calculate the mean value of SMB in the western and eastern regions of the West Antarctic, we first derived the mean SMB of all these ice cores in this location (within a 25 km range).

We use the monthly SST data from the Hadley Centre sea ice and sea surface temperature data set (HadISST) (Rayner et al., 2003) with a spatial resolution of 1°x1°. The monthly SST data during 1980-2010 is used to calculate SST trends over the three ocean basins (the Pacific, Atlantic and Indian Ocean), as well as the tropical SST time series. Additionally, the SST data is also used as a boundary condition in the atmospheric model experiments detailed below. The tropical Pacific SST anomaly is measured by Nino3.4 index, the SST anomaly in the central-eastern tropical Pacific region (5°S–5°N, 170°–120°W). The tropical Atlantic SST anomaly is measured by the mean SST in the tropical Atlantic from 20°S to 20°N (TA20). The SST anomaly in the tropical Indian Ocean is measured by the Indian Ocean basin mode (IOBM) index (Xie et al., 2009), which is defined as the mean SST in the tropical Indian Ocean from 20°S to 20°N. The SST variability indices in the three ocean basins are derived from monthly SST in the HadISST dataset.

2.1.2 Atmospheric reanalysis datasets

Atmospheric reanalysis datasets, while providing comprehensive spatial and temporal coverage of precipitation data, offer reliable insights predominantly in the satellite era, post-1980 (Hersbach et al., 2020). To evaluate SMB changes in

https://doi.org/10.5194/egusphere-2025-1381
Preprint. Discussion started: 21 May 2025

West Antarctica, we analyze precipitation and evaporation data from five reanalysis datasets for the period 1980–2010: the European Center for Medium-Range Weather Forecasts Reanalysis version 5 (ERA5) (Hersbach et al., 2020), the Japanese 55-year Reanalysis (JRA55) (Kobayashi et al., 2015), the Climate Forecast System Reanalysis (CFSR) (Saha et al., 2010), the Modern-Era Retrospective analysis for Research and Applications version-2 (MERRA2) (Gelaro et al., 2017), the NCEP-DOE Reanalysis version-2 (NCEP2) (Kanamitsu et al., 2002). These datasets originally feature varying resolutions: 0.25°x0.25° for ERA5, nominally 0.56°x0.56° for JRA55, 0.312°x0.312° for CFSR, 0.5°x0.625° for MERRA2 and 2.5°x2.5° for NCEP2. To facilitate comparisons, all data are interpolated into a uniform resolution of 0.5°x0.5° using the bilinear interpolation method. Other variables, geopotential height, vertically integrated moisture transport and its divergence from ERA5 are used to investigate the underlying mechanisms driving changes in SMB over West Antarctica.

2.2 Methods

2.2.1 Statistical methods

Ordinary least squares regression is used to evaluate the individual contribution of SST variabilities in the three ocean basins on SMB changes in West Antarctica. The adjusted Student's *t*-test is used to determine the confidence intervals for regression coefficients (Bretherton et al., 1999), accounting for autocorrelation in climate data. The degrees of freedom (T) are adjusted into (T^*) as Eq. (1):

$$T^* = T(1 - r_1 r_2)/(1 + r_1 r_2), \quad (1)$$

where r_1 and r_2 are the lag-one autocorrelations of the climate variables' time series in each grid and the SST indices of the three ocean basins, respectively.

Sen's slope method (Gocic and Trajkovic, 2013) is used to calculate the trends in SMB in ice core records, precipitation, evaporation and geopotential height in reanalysis and model data described below, with the confidence intervals estimated through the Mann-Kendall test (Gocic and Trajkovic, 2013).

2.2.2 Model simulation

We use the global atmosphere model, Community Atmosphere Model version 5 (CAM5), developed by National Center for Atmospheric Research (NCAR), to analyze the individual impact of the decadal SST changes in the three ocean basins, Atlantic, Pacific and Indian Oceans on the observed trends in SMB over West Antarctica. We conduct modeling experiments using a finite volume grid at 1.9°x2.5° horizontal resolution. The model is driven by SST as lower external boundary forcing. We also use the Community Land Model and the thermodynamic module of the Community Sea-Ice Model to simulate the surface heat and moisture fluxes.

Three groups of transient CAM5 ensemble simulations are forced by observed time-varying (with trend) SST over the Pacific (40°S~65°N), Atlantic (30°S~75°N) and Indian (25°S ~ 25°N) Oceans, respectively, for the period 1980–2010. Each

https://doi.org/10.5194/egusphere-2025-1381
Preprint. Discussion started: 21 May 2025

group of ensemble simulations comprises 12 members based on different perturbed initial conditions. To prevent spurious boundary effects, SST anomalies were gradually reduced to zero using linear interpolation, which ensures a smooth transition within a defined buffer zone (10° in latitude and longitude). In other regions, SST and sea ice are set to their climatological mean states (1981-2010) with an annual cycle. During the entire integration period, other forcings, including greenhouse gas concentrations, aerosols, and solar radiation, remain constant throughout the integration period. The ensemble means of all members are calculated to represent the climate response to the SST forcing from each ocean basin by minimizing the noise from the internal variabilities of the atmosphere.

3 Results

3.1 Dipole-like surface mass balance trends in West Antarctica

3.1.1 Annual-mean surface mass balance trends

The ice core records reveal a clear dipole-like pattern of SMB trends in West Antarctica (**Fig. 1a**), characterized by decreasing trends in the western region and increasing trends in the eastern region. We calculated the mean trends by calculating the average of all ice core records within the western and eastern regions. The results show a decrease in SMB of -22.6±16.6 kg m^{-2} yr^{-1} $decade^{-1}$ (p-value = 0.0005) (**Fig. 1b**) in the west and an increase of 96.0±86.2 kg m^{-2} yr^{-1} $decade^{-1}$ (p-value = 0.02) (**Fig. 1c**) in the east, both significant at the 95% confidence level. Net precipitation (precipitation minus evaporation) in reanalysis datasets during the satellite era is reported to well represent the Antarctic SMB (Medley and Thomas, 2019; Wang et al., 2016). As a reference, we calculate the SMB trends from 1980 to 2010, using ERA5 data. The results also show a dipole-like trend pattern, as revealed by the ice core records, with decreasing trends in the west and increasing trends in the east (**Fig. 1a**). The coastal region and the Antarctic Peninsula exhibit larger trends than the interior of West Antarctica because the coastal regions are more sensitive to the moisture transport from the Southern Ocean (Clem et al., 2016; Ding and Steig, 2013).

https://doi.org/10.5194/egusphere-2025-1381
Preprint. Discussion started: 21 May 2025

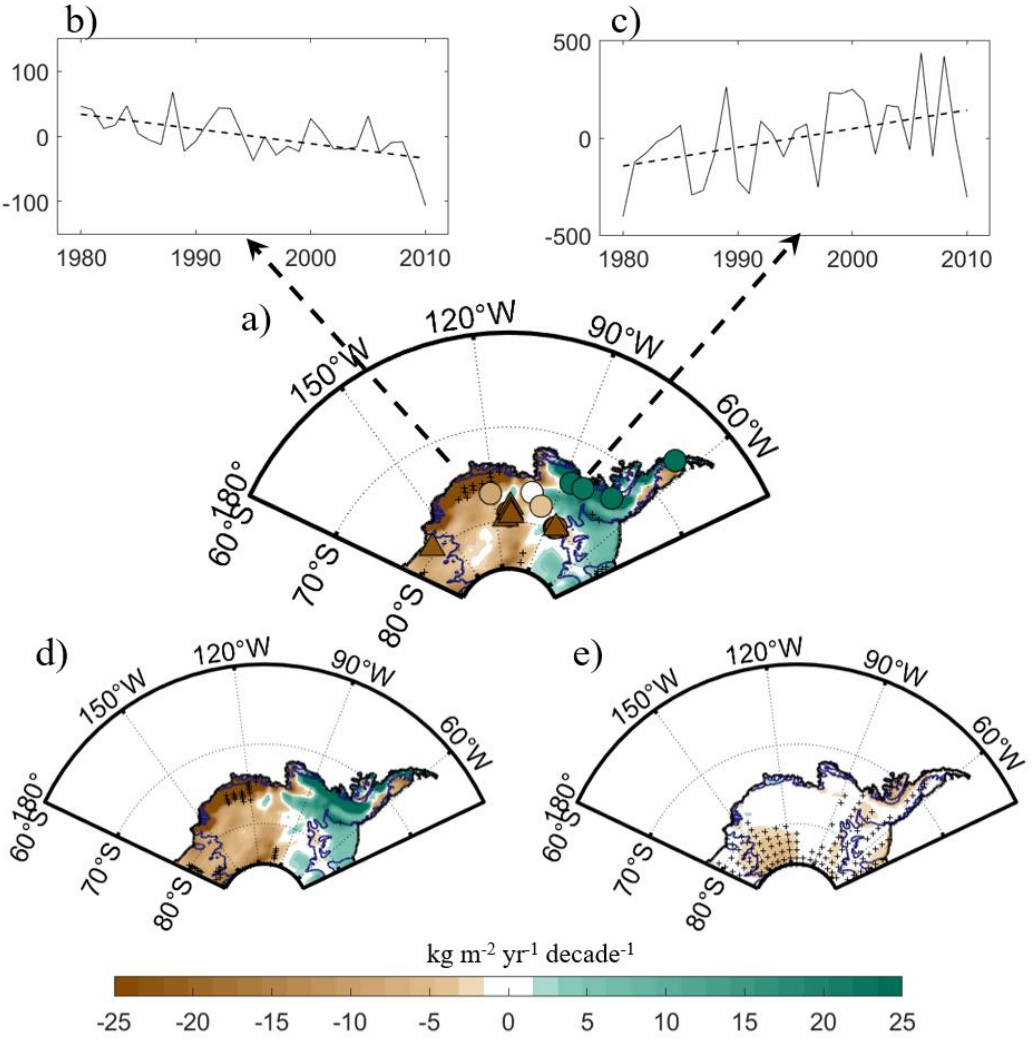

Figure 1 | Surface mass balance trends in West Antarctica during 1980-2010. a shows the net precipitation (precipitation minus evaporation) trends in ERA5. The colored circles and triangles show the SMB trend for each ice core records, with the significant trends shown by triangles. **b** and **c** show the SMB time series of stacked ice core records (solid line) in the western (**b**) and the eastern part (**c**) of West Antarctica, respectively. In **b** and **c**, the dashed line indicates the linear trend in SMB. **d** and **e** show the precipitation and negative evaporation (multiplied by -1) trends, respectively. Black crosses show the area with statistically significant trends.

Considering the uncertainty of the reanalysis datasets over the South Pole region, we evaluate the SMB trends using four additional state-of-the-art reanalysis datasets (JRA55, CFSR, MERRA2 and NCEP2). All four datasets consistently reveal a similar dipole-like trend pattern of the SMB over West Antarctica (**Fig. 2**), even if MERRA2 and NCEP2 show relatively weaker decreasing trends in the western part (**Fig. 2c and d**). The consistency between the ice core records and the five reanalysis datasets highlights the robustness of the dipole-like SMB trends over the West Antarctic Ice Sheet.

We further single out the contributions of the precipitation and evaporation in the SMB trends over West Antarctica. The precipitation trend pattern is nearly identical to that of the SMB (**Fig. 1d**). However, the evaporation across the West

https://doi.org/10.5194/egusphere-2025-1381
Preprint. Discussion started: 21 May 2025

Antarctic Ice Sheet has increased (**Fig. 1c** shows the negative trends) with a distinct pattern and magnitude from that of the SMB. In the rest of the study, we thus mainly focus on the precipitation trends over West Antarctica.

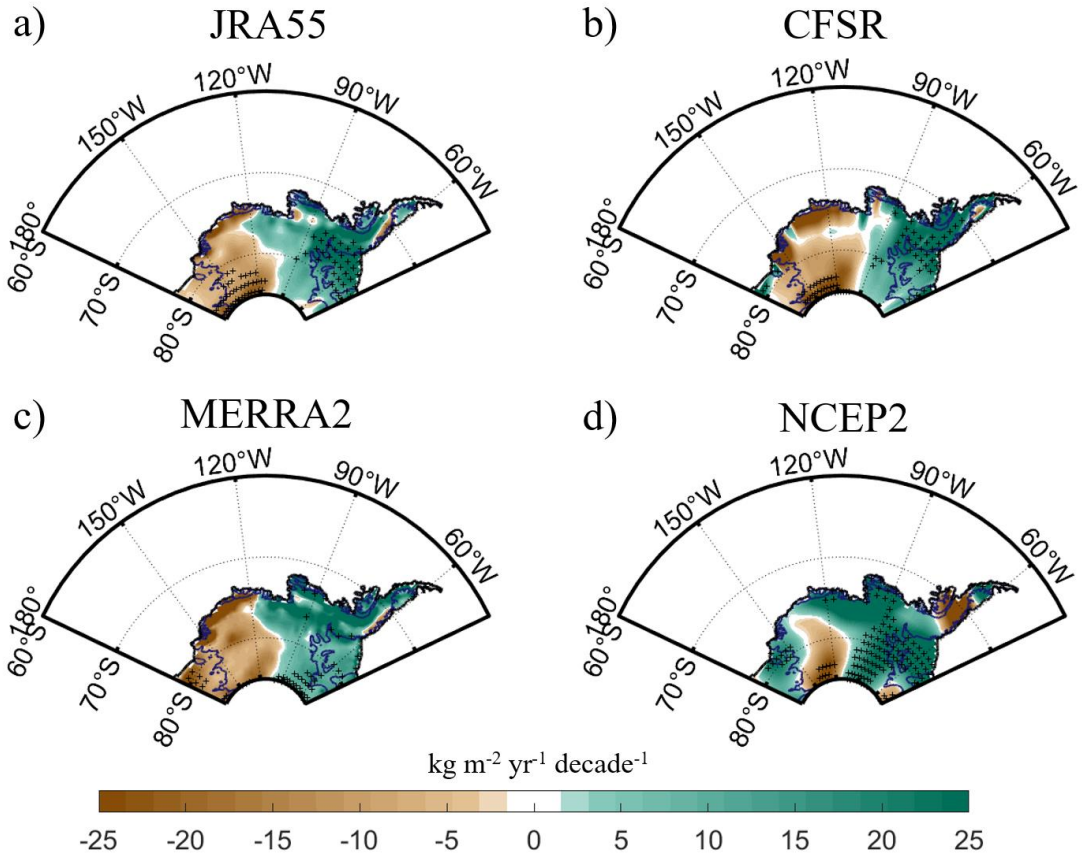

Figure 2 | Net precipitation trends in the other four reanalysis datasets. a-d show the net precipitation trends in JRA55 (**a**), CFSR (**b**), MERRA2 (**c**) and NCEP2 (**d**), respectively. Black crosses show the area with statistically significant trends.

3.1.2 Seasonality of the West Antarctic precipitation trends

Precipitation in West Antarctica has strong seasonality (Oshima and Yamazaki, 2006). To estimate the seasonal contributions to the overall SMB trends, we evaluate the seasonal precipitation trends using ERA5 data. Precipitation in austral spring (SON), summer (DJF) and autumn (MAM) shows a similar dipole-like trend pattern (**Fig. 3**) as that of the annual trends, although the decreasing trends during SON in West Antarctica's western region are relatively weak (**Fig. 3d**). However, the winter (JJA) precipitation exhibits decreasing trends over almost the entire Western Antarctica except for the inland region of its western part (**Fig. 3c**), which is the only season without a dipole-like precipitation pattern.

https://doi.org/10.5194/egusphere-2025-1381
Preprint. Discussion started: 21 May 2025

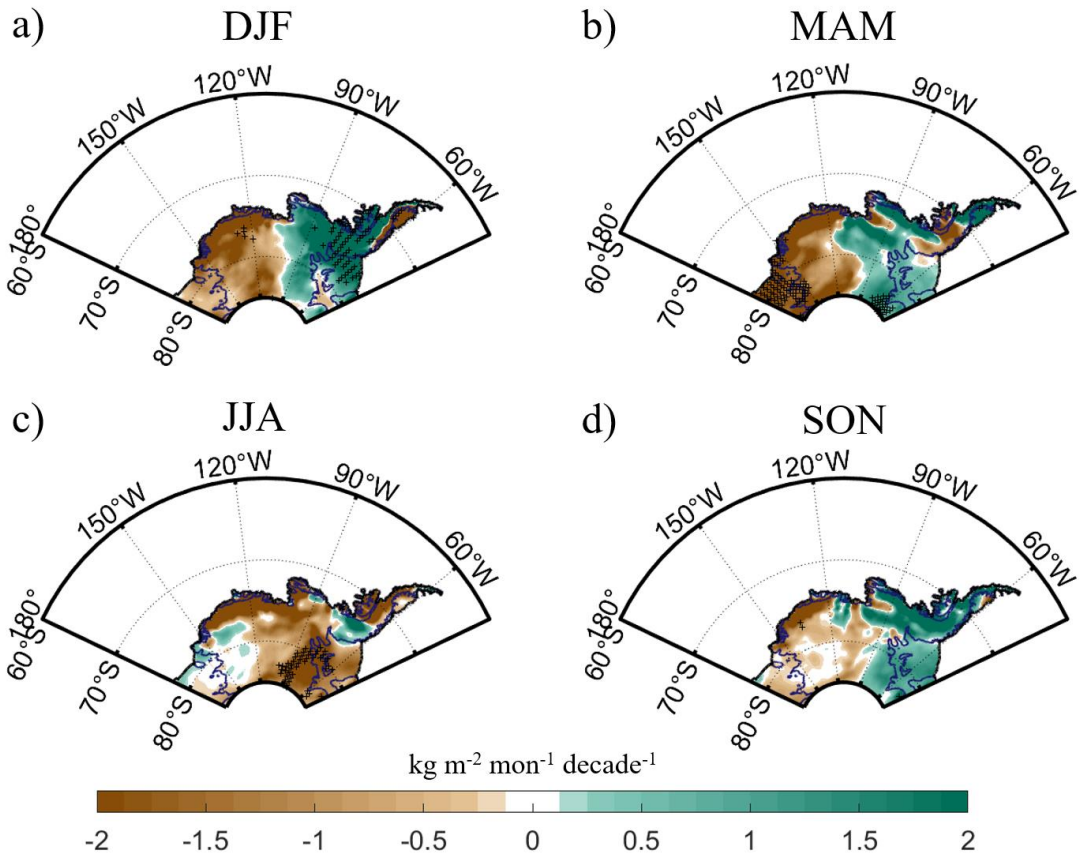

Figure 3 | Precipitation trends in ERA5 for each season. a shows the trends in austral summer (December to February, DJF). **b** shows the trends in autumn (March to May, MAM). **c** shows the trends in winter (June to August, JJA). **d** shows the trends in spring (September to November, SON). Black dots show the area with statistically significant trends.

To validate the seasonality of precipitation trends identified in ERA5 data, its trends for each season are analyzed using four additional reanalysis datasets individually, with the results shown in Figure 4. Results based on all four reanalysis datasets show a clear dipole-like pattern of the precipitation trends over West Antarctica in austral spring (SON), summer (DJF), and autumn (MAM), with an increase over western West Antarctica and a decrease over the east (**Fig. 4**). During JJA, however, the precipitation trends in CFSR and NCEP2 show an increasing pattern (**Fig. 4g** for CFSR) and decreasing pattern over the entire West Antarctic (**Fig. 4o** for NCEP2), respectively. This result highlights the high JJA precipitation uncertainty in West Antarctica, although it does not influence our main conclusion.

https://doi.org/10.5194/egusphere-2025-1381
Preprint. Discussion started: 21 May 2025

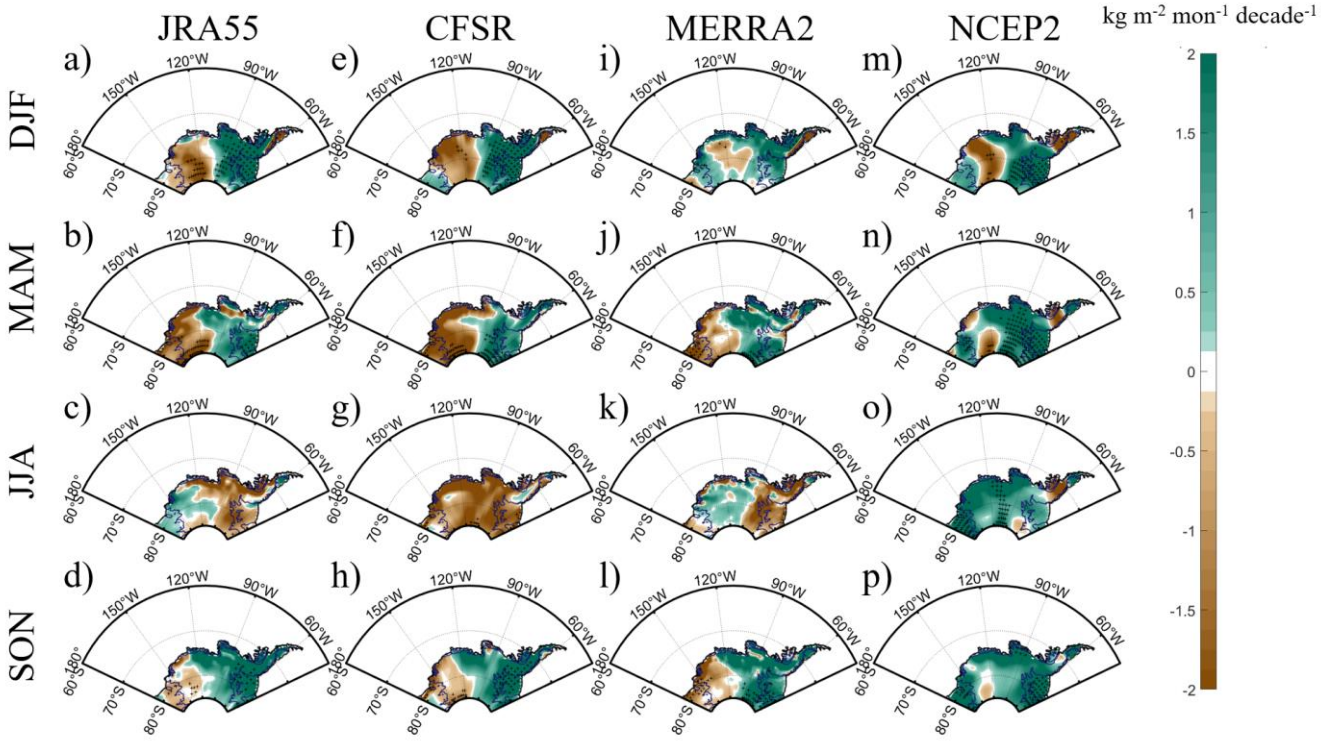

Figure 4 | Seasonal precipitation trends in the other four reanalysis datasets. a-d show the precipitation trends in austral summer (**a**, December to February, DJF), autumn (**b**, March to May, MAM), winter (**c**, June to August, JJA) and spring (**d**, September to November, SON) in JRA55. **e-h** show the precipitation trends in CFSR. **i-l** show the precipitation trends in MERRA2. **m-p** show the precipitation trends in NCEP2. Black crosses show the area with statistically significant trends.

Combining the ice core records and the five reanalysis datasets, we demonstrate robust dipole-like SMB trends in West Antarctica, marked by decreases in the west and increases in the east. Seasonal analysis further reveals that the precipitation trends in DJF, MAM and SON contribute to this dipole-like trend pattern. In addition, the JJA precipitation trends appear to show decreases over the entire West Antarctica. In the rest of the study, we further investigate the role of tropical teleconnections in these SMB trend patterns, as well as their driving mechanisms.

3.2 West Antarctic surface mass balance pattern associated with tropical SST variabilities

During 1980-2010, muti-decadal trends in tropical SST are characterized by a positive phase of AMO and a negative phase of IPO, with strong warming trends over the tropical Atlantic and Indian Ocean but mild cooling trends over the eastern tropical Pacific Ocean (**Fig. 5**). Importantly, these tropical SST trends also show clear seasonality. The surface cooling over the eastern tropical Pacific is much weaker in JJA (-0.03±0.24 ℃ decade^{-1} in Nino3.4 region) compared to that of any other season (average of -0.10±0.35 ℃ decade^{-1}). The tropical Atlantic warming trend is significant in DJF, MAM and SON (average of 0.19±0.13 ℃ decade^{-1} in 10°S~10°N), but weaker and insignificant in JJA (0.17±0.19 ℃ decade^{-1}). The tropical Indian Ocean shows the strongest and most significant warming trends in JJA (0.10±0.09 ℃ decade^{-1} in

https://doi.org/10.5194/egusphere-2025-1381
Preprint. Discussion started: 21 May 2025

20°S~20°N), but weaker and non-significant trends in SON (0.09±0.10 °C decade^{-1}) and MAM (0.09±0.09 °C decade^{-1}). These seasonal changes in tropical SST over the past decades stimulate tropical-polar atmospheric teleconnections, further influencing the seasonality of the SMB trends in the West Antarctic Ice Sheet.

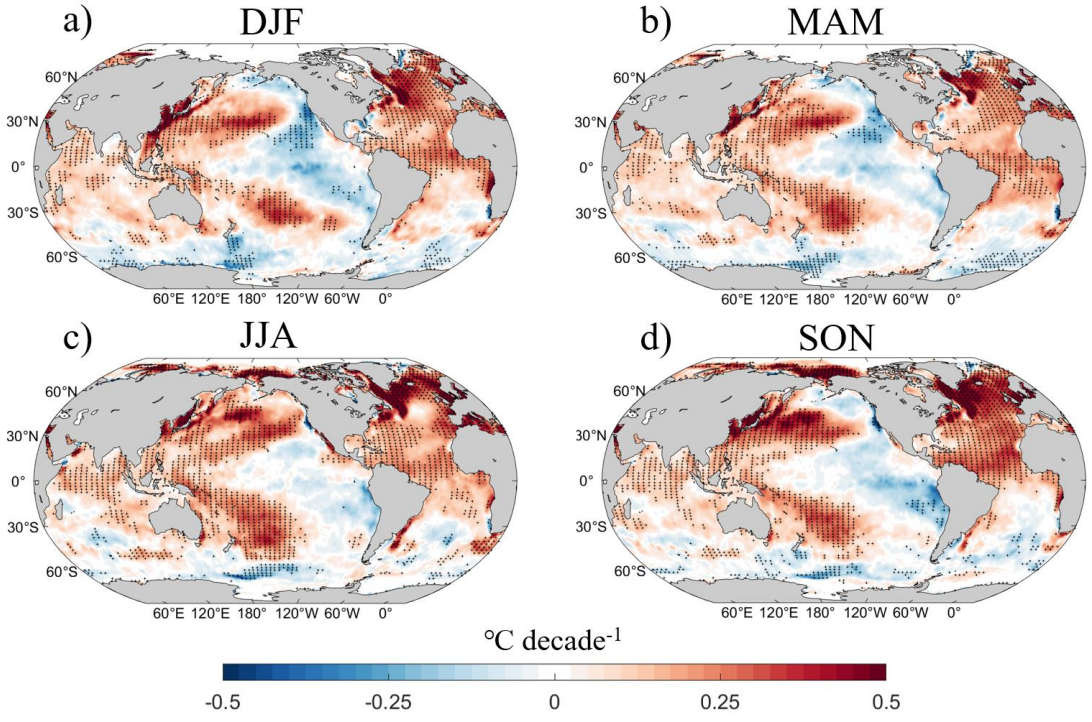

Figure 5 | Sea surface temperature trends for each season during the period of 1980-2010. a shows the trends in austral summer (December to February, DJF) derived from HadISST. **b** shows the trends in autumn (March to May, MAM). **c** shows the trends in winter (June to August, JJA). **d** shows the trends in spring (September to November, SON). Black crosses show the area with statistically significant trends.

To single out the influence of each ocean basin on the West Antarctic SMB, we regress the SMB in ice core records and the annual precipitation in ERA5 against tropical SST indices, Nino3.4 (negative, representing the contribution of tropical Pacific cooling trends), TA20 and IOBM. The results indicate that the dipole-like SMB pattern in West Antarctica is associated with both eastern tropical Pacific cooling and tropical Atlantic warming (**Fig. 6a and f**). Specifically, one standard deviation in tropical Pacific cooling corresponds to a decrease of about 1.5 kg m^{-2} mon^{-1} in precipitation in western West Antarctica and an increase of over 1.8 kg m^{-2} mon^{-1} in the east (**Fig. 6a**). Likewise, one standard deviation in tropical Atlantic warming is linked to a decrease of more than 2.5 kg m^{-2} mon^{-1} in the west and an increase of over 3.8 kg m^{-2} mon^{-1} in the east (**Fig. 6f**). On the other hand, based on the ice core records, the Indian Ocean warming appears to be related to a decrease in SMB over the entire West Antarctic, although the Indian Ocean warming - associated precipitation anomalies are much smaller in ERA5 data, in comparison to that of ice core records (**Fig. 6k**).

https://doi.org/10.5194/egusphere-2025-1381
Preprint. Discussion started: 21 May 2025

The regression results suggest that the dipole-like trend pattern in the West Antarctic SMB is potentially driven by eastern tropical Pacific cooling and tropical Atlantic warming trends. Still, the seasonality of these teleconnection patterns has not been analyzed. We thus regress the precipitation against tropical SST indices for each season to evaluate the seasonal contribution of each ocean basin on the dipole-like precipitation trends in West Antarctica. The results indicate that the Pacific Ocean may drive the dipole-like patterns in all four seasons (**Fig. 6b-e**). Likewise the Atlantic Ocean triggers dipole-like patterns in all seasons, except for DJF (**Fig. 6g-j**). Nonetheless, during MAM, the regression coefficients for both the Pacific and Atlantic Oceans are more pronounced in the western part of West Antarctica (**Fig. 6c and h**). In JJA, the regression results for these two ocean basins both show dipole-like patterns (**Fig. 6d and i**), but considering the weakest tropical SST trends in JJA over both the tropical Pacific and Atlantic, these teleconnections may contribute less to the dipole-like precipitation pattern in JJA compared to other seasons. In contrast, during JJA, the Indian-Ocean-warming-related teleconnections may dramatically decrease the precipitation over the eastern part of West Antarctica (**Fig. 6n**), resembling the precipitation trend pattern in ERA5 (**Fig. 3c**), as well as those in JRA55 (**Fig. 4c**) and MERRA2 (**Fig. 4k**).

https://doi.org/10.5194/egusphere-2025-1381
Preprint. Discussion started: 21 May 2025

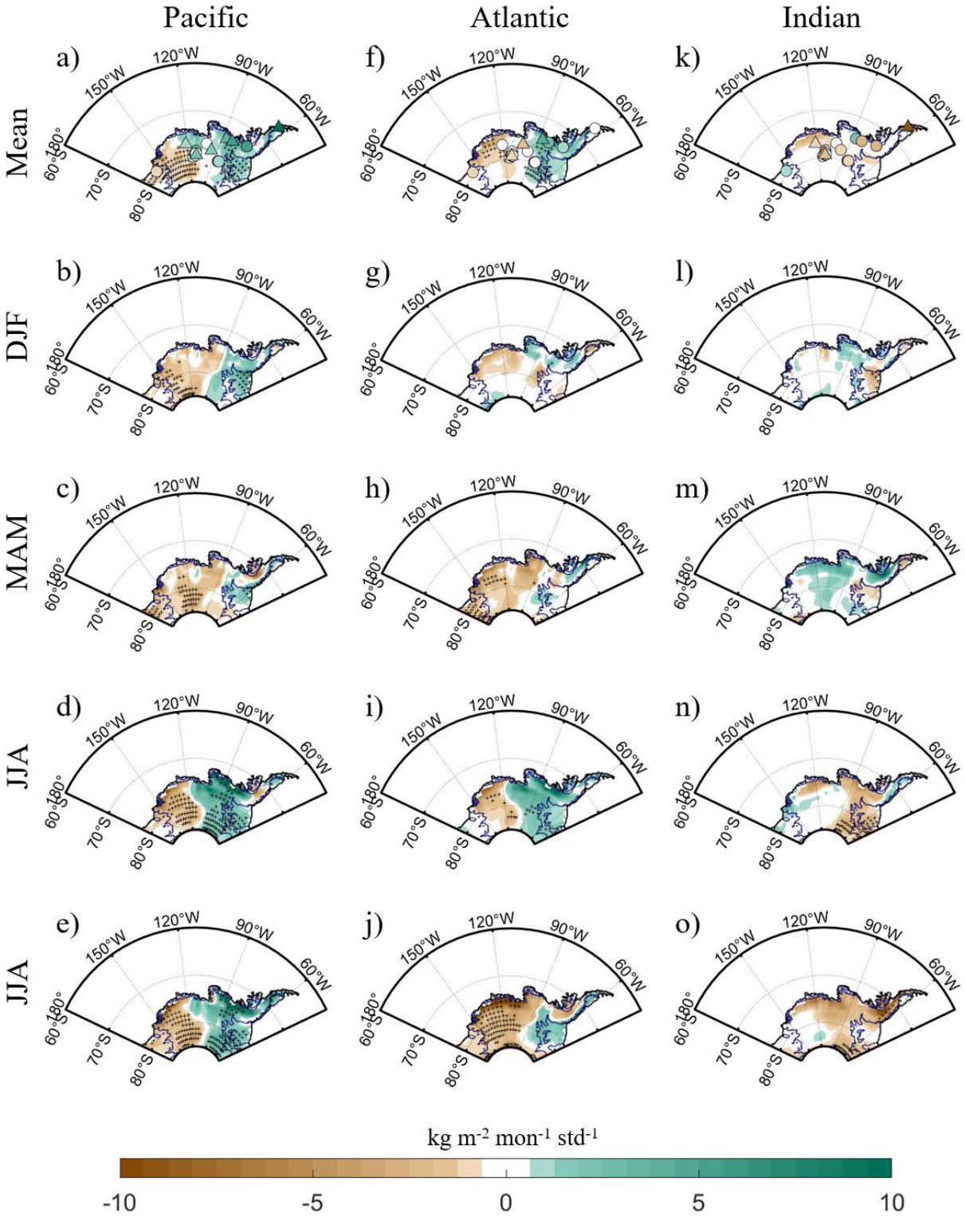

https://doi.org/10.5194/egusphere-2025-1381
Preprint. Discussion started: 21 May 2025

Figure 6 | Annual and seasonal patterns of regression coefficients of precipitation against sea surface temperature indices in three ocean basins. a-e show the annual (**a**) and seasonal regression patterns against Nino3.4 in austral summer (**b**, December to February, DJF), autumn (**c**, March to May, MAM), winter (**d**, June to August, JJA) and spring (**e**, September to November, SON). **f-j** show the regression patterns against TA20. **k-o** show the regression patterns against IOBM. Black crosses show the area where the regression coefficients are statistically significant. The precipitation data are derived from ERA5.

Through the regression analysis, we demonstrate that both the eastern tropical Pacific cooling and tropical Atlantic warming contribute to the dipole-like SMB trends in West Antarctica. Further analysis of seasonality reveals that the tropical Pacific and Atlantic Ocean may contribute to the dipole-like SMB trends in MAM and SON, while the Indian Ocean may contribute to the precipitation trends in JJA. Additionally, the tropical Pacific may also contribute to the dipole-like precipitation trends in DJF to some extent, although the Southern Hemispheric atmospheric circulation anomalies for DJF are largely attributed to ozone depletion and recovery (Lenaerts et al., 2018). The above analysis reveals significant linkages between the three tropical oceans and the West Antarctic SMB. However, the underlying mechanisms remain unclear, which is the main focus of the rest of this study.

3.3 Atmospheric bridges linking the tropical oceans and the Antarctic precipitation

We further analyze the physical pathway through which the tropical oceans drive the precipitation changes over West Antarctica. Given that atmospheric circulation adjustment usually links the tropical SST and higher-latitudes climate variabilities, we regress the 500hPa geopotential height against Nino3.4 (negative), TA20 and IOBM (**Fig. 7**). The Nino3.4-associated regression patterns show deepened ASL through Pacific-Southern American (PSA)-like patterns extending from the subtropical central Pacific to West Antarctica in all four seasons (**Fig. 7a-d**). In MAM (**Fig. 7b**), JJA (**Fig. 7c**) and SON (**Fig. 7d**), the anomalous low-pressure center is more localized near the West Antarctic. In DJF, central-eastern Pacific cooling is nonetheless associated with an intensified SAM, with low-pressure anomaly over the entire Antarctic (**Fig. 7a**). The TA20-associated regression patterns (**Fig. 7e-h**) also show deepened ASL in MAM (**Fig. 7f**), JJA (**Fig. 7g**) and SON (**Fig. 7h**). However, in DJF, a weak high-pressure anomaly appears around West Antarctica (**Fig. 7e**). This weakening of Atlantic – Antarctic teleconnection is primarily attributed to the weakened sub-tropical jet (Southern Hemisphere) in DJF, which fails to guide the Rossby wave train stimulated by tropical Atlantic warming(Li et al., 2015). In contrast, the IOBM-associated regression patterns show anomalous high-pressure centers around West Antarctica for all four seasons, albeit the location of the circulation centers differ between seasons (**Fig. 7i-l**). The atmospheric circulation adjustment induced by the cooling of the eastern tropical Pacific Ocean, and the warming of the tropical Atlantic and Indian Ocean may further influence moisture transport from the ocean towards the West Antarctic Ice Sheet, potentially affecting the SMB over there.

https://doi.org/10.5194/egusphere-2025-1381
Preprint. Discussion started: 21 May 2025

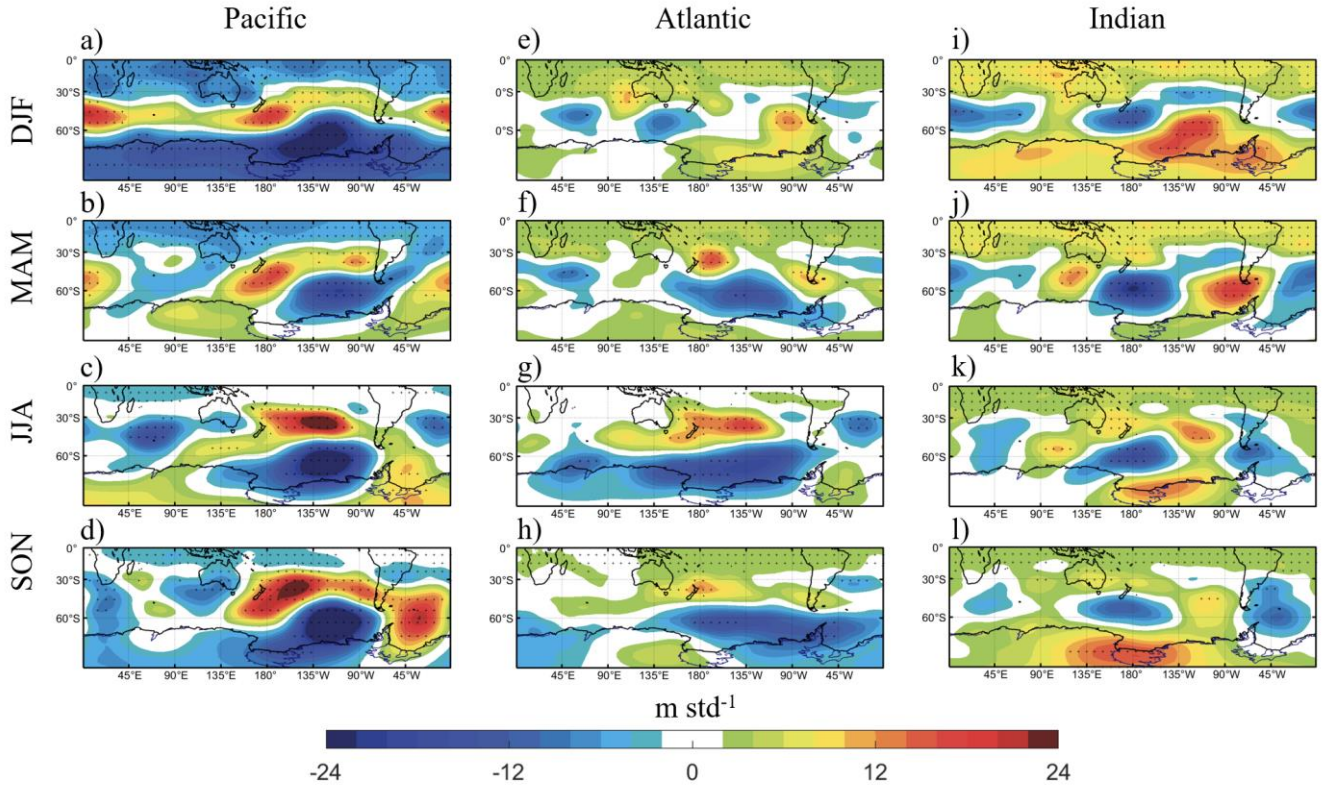

Figure 7 | Regression patterns of 500hPa geopotential height against sea surface temperature indices in the tropical Pacific and Atlantic Ocean for each season. a-d show the regression patterns against Nino3.4 in austral summer (**a**, December to February, DJF), autumn (**b**, March to May, MAM), winter (**c**, June to August, JJA) and spring (**d**, September to November, SON). **e-h** show the regression patterns against TA20. **i-l** show the regression patterns against IOBM. Black crosses show the area where the regression coefficients are statistically significant. The 500 hPa geopotential height data are from ERA5.

We further examine the regression of vertically integrated horizontal moisture transport and associated moisture divergence over West Antarctica against Nino3.4 (negative), TA20 and IOBM. The regression results show that the deepened ASL, triggered by eastern tropical Pacific cooling and tropical Atlantic warming, transports additional moisture from the Southern Ocean to the western part of West Antarctica, while the eastern part is dominated by dry southerly wind from inland (**Fig. 8a-h**). Subsequently, the moisture transport anomaly leads to the moisture convergence in the east due to the orographic lifting and adiabatic cooling (Bromwich, 1988), and leads to the moisture divergence in the west, aligning with the dipole-like pattern in precipitation. Conversely, the high-pressure anomaly induced by the tropical Indian Ocean warming, particularly in the JJA (**Fig. 8k**), mainly leads to an out-of-land moisture transport in West Antarctica, resulting in anomalous moisture divergence and thus a reduction of precipitation.

https://doi.org/10.5194/egusphere-2025-1381
Preprint. Discussion started: 21 May 2025

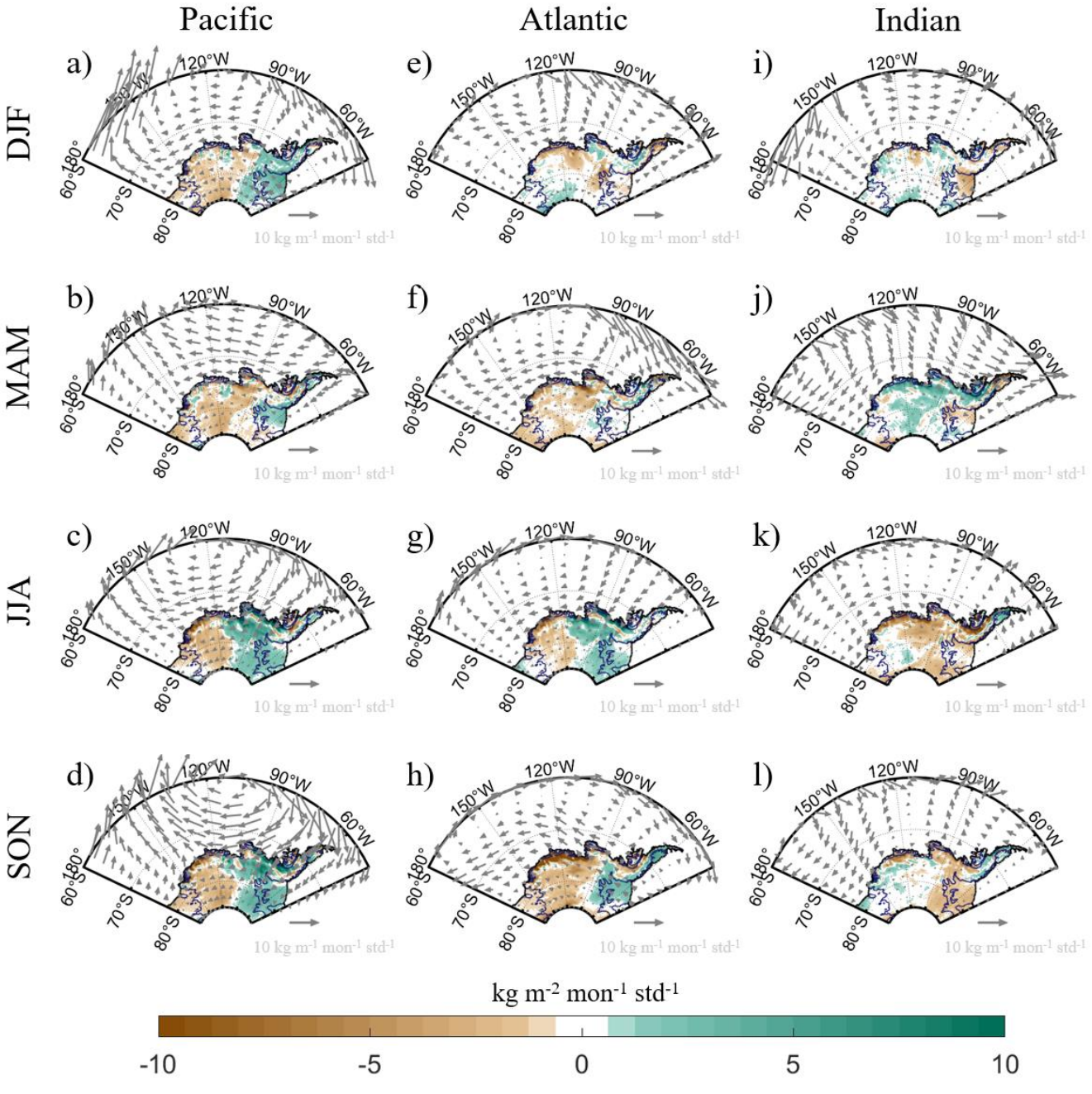

Figure 8 | Seasonal patterns of regression coefficients of moisture transports (vector) and their convergence (color shading). a-d show the regression patterns against Nino3.4 in austral summer (**a**, December to February, DJF), autumn (**b**, March to May, MAM), winter (**c**, June to August, JJA) and spring (**d**, September to November, SON). **e-h** show the regression patterns against TA20. **i-l** show the regression patterns against IOBM. The moisture transports data are derived from ERA5.

https://doi.org/10.5194/egusphere-2025-1381
Preprint. Discussion started: 21 May 2025

The regression results of atmospheric circulation demonstrate that the eastern tropical Pacific cooling and the tropical Atlantic warming both stimulate Rossby wave trains, thus intensifying the ASL around West Antarctica in DJF, MAM and SON. In contrast, the Rossby wave trains aroused by the Indian Ocean warming weaken the ASL in all four seasons. In DJF, MAM and SON, the deepened ASL associated with SST changes in the tropical Pacific and Atlantic Ocean further lead to additional moisture transport from the Southern Ocean towards eastern West Antarctica, but drive cold and dry wind from the inland Antarctic to the western part of West Antarctica, resulting in the contrasting anomalous moisture convergence between these two regions. For JJA, the Indian-Ocean-warming-induced circulation anomaly drives a southerly wind over the entire West Antarctic, partly contributing to the decreased precipitation during that season.

3.4 Model simulations

The regression analysis reveals the relationship between tropical SST variabilities in the three ocean basins and the precipitation patterns in West Antarctica, but the causality has not been fully clarified. To investigate the causal links between SST trends and the West Antarctic precipitation trends, we perform three sets of atmospheric model experiments using CAM5, isolating the effects of SST trends in the Pacific, Atlantic, and Indian Oceans during 1980–2010 by prescribing observed time-varying SSTs in each basin while keeping other forcings constant (see methods, Section 2.2.2).

To validate the tropical-polar teleconnections revealed by the regression analysis, we first examine the simulated 500hPa geopotential height trends (**Fig. 9**). Both the tropical eastern Pacific cooling and the tropical Atlantic warming intensify the ASL through atmospheric teleconnections in MAM (**Fig. 9b and f**) and SON (**Fig. 9d and h**), while the Indian Ocean warming drives high-pressure center around West Antarctica in JJA (**Fig. 9k**), which all align with the regression analysis findings. Nevertheless, the low-pressure center over West Antarctica induced by the Pacific Ocean is relatively weaker compared to the regression analysis (**Fig. 9a**). Overall, the simulated atmospheric circulation anomalies corroborate most of the features revealed by the regression analysis.

https://doi.org/10.5194/egusphere-2025-1381
Preprint. Discussion started: 21 May 2025

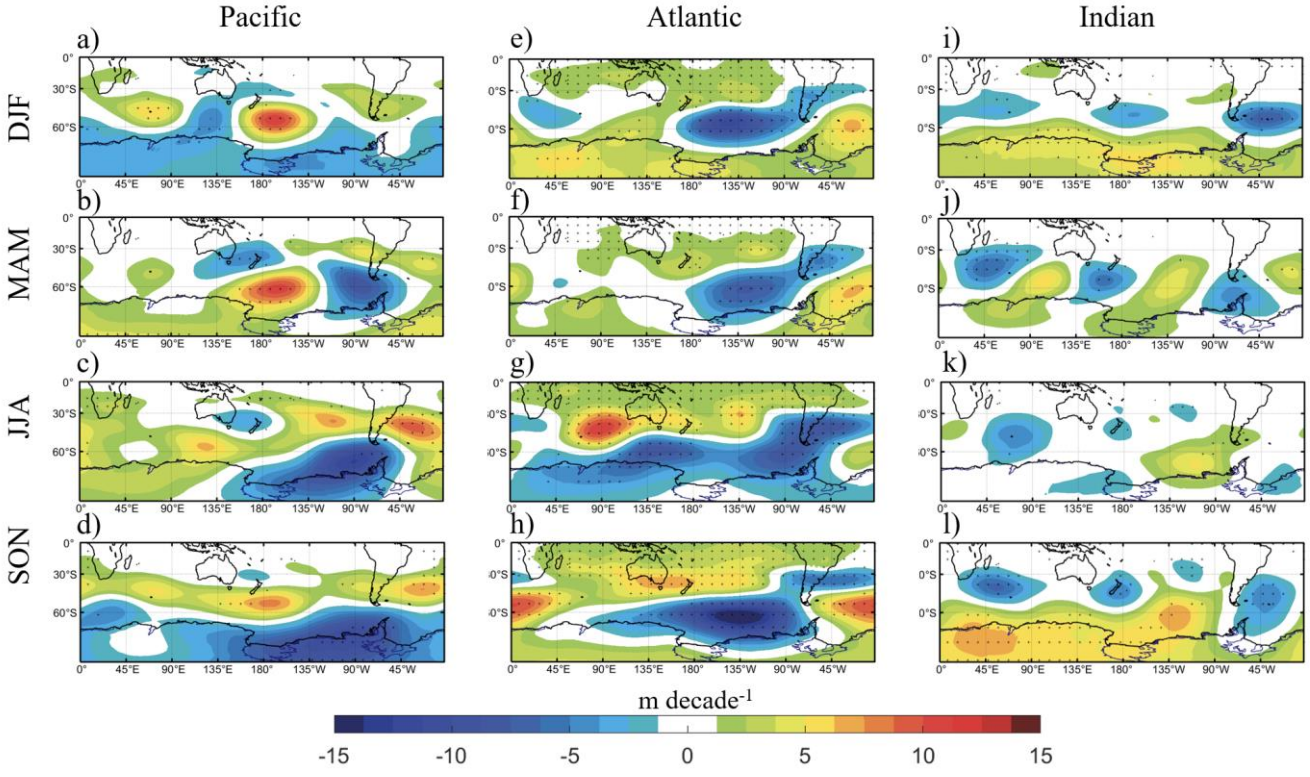

Figure 9 | Simulated response of 500hPa geopotential height trends to observed SST in three ocean basins during 1980-2010. a-d show the response to Pacific SST in austral summer (**a**, December to February, DJF), autumn (**b**, March to May, MAM), winter (**c**, June to August, JJA) and spring (**d**, September to November, SON). **e-h** show the response to Atlantic SST. **c-l** show the response to Indian Ocean SST. Black crosses show the area with statistically significant trends. Details about the simulated data are provided in the methods section (Section 2.2.2).

We further calculate the simulated moisture transport and associated moisture divergence trends (**Fig. 10**). The deepened ASL in DJF (**Fig. 10a and e**), MAM (**Fig. 10b and f**) and SON (**Fig. 10d and h**) forced by Pacific and Atlantic SST changes lead to the moisture transport towards eastern West Antarctica. At the same time, they drive cold and dry air from inland Antarctica to the western part of West Antarctica, resulting in the moisture convergence in the east and divergence in the west. In DJF, the moisture transports forced by the Pacific Ocean mainly induce moisture convergence in the eastern West Antarctica. For the Indian Ocean, typically in JJA (**Fig. 10k**), the high-pressure anomaly induces moisture transport from the ocean to western West Antarctica but reduces it to the east, as well as the associated moisture convergence in the west and divergence in the east.

https://doi.org/10.5194/egusphere-2025-1381
Preprint. Discussion started: 21 May 2025

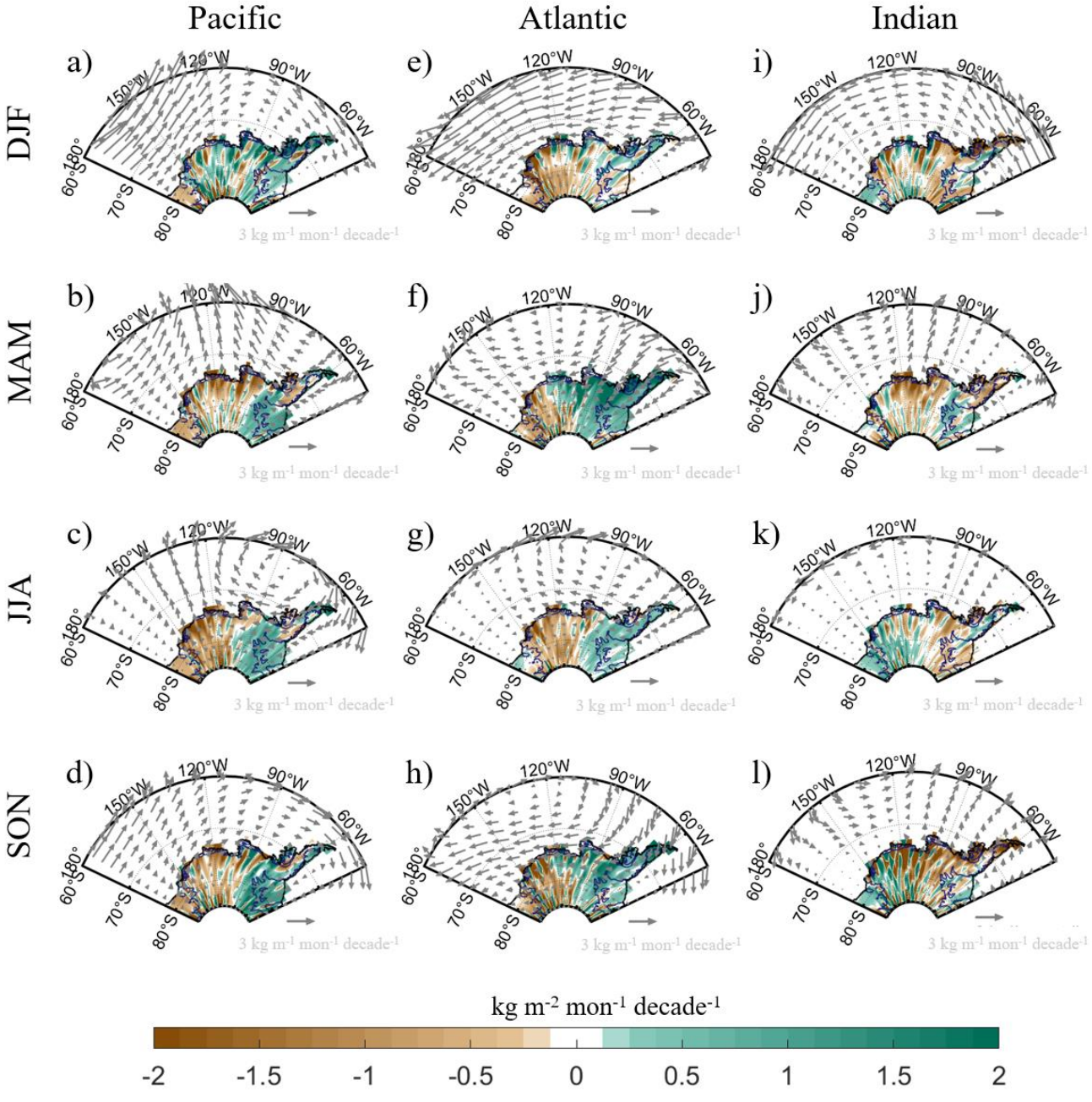

Figure 10 | Simulated response of moisture transports (vector) and their divergence (color shading) trends to observed SST in three ocean basins. a-d show the response to Pacific SST in austral summer (**a**, December to February, DJF), autumn (**b**, March to May, MAM), winter (**c**, June to August, JJA) and spring (**d**, September to November, SON). **e-h** show the response to Atlantic SST. **i-l** show the response to Indian Ocean SST. Details about the simulated data are provided in the methods section (Section 2.2.2).

https://doi.org/10.5194/egusphere-2025-1381
Preprint. Discussion started: 21 May 2025

Finally, we calculate the model response of the precipitation trends for each experiment. In the Pacific and Atlantic simulations, the results show clear dipole-like precipitation trend patterns, consistent with the trend patterns in reanalysis datasets and regression patterns against SST indices. In particular, the simulation results in DJF (**Fig. 11a and e**), MAM (**Fig. 11b and f**) and SON (**Fig. 11d and h**) show increasing precipitation trends in eastern West Antarctica and decreasing trends in the west, although the DJF precipitation trend forced by the Pacific Ocean manifests as a significant and stronger increasing pattern over eastern West Antarctica. On the other hand, for the Indian Ocean, particularly in JJA (**Fig. 11k**), our result shows a decreasing precipitation trend in the eastern West Antarctica, consistent with the regression results of IOBM, as well as the West Antarctic precipitation trend in most of the reanalysis datasets during JJA.

Overall, the simulated precipitation trends align well with observed ones, exhibit similar patterns to the regression analysis using observed data, highlighting that tropical Pacific and Atlantic SST forcing primarily drive the dipole-like precipitation trends in West Antarctic.

https://doi.org/10.5194/egusphere-2025-1381
Preprint. Discussion started: 21 May 2025

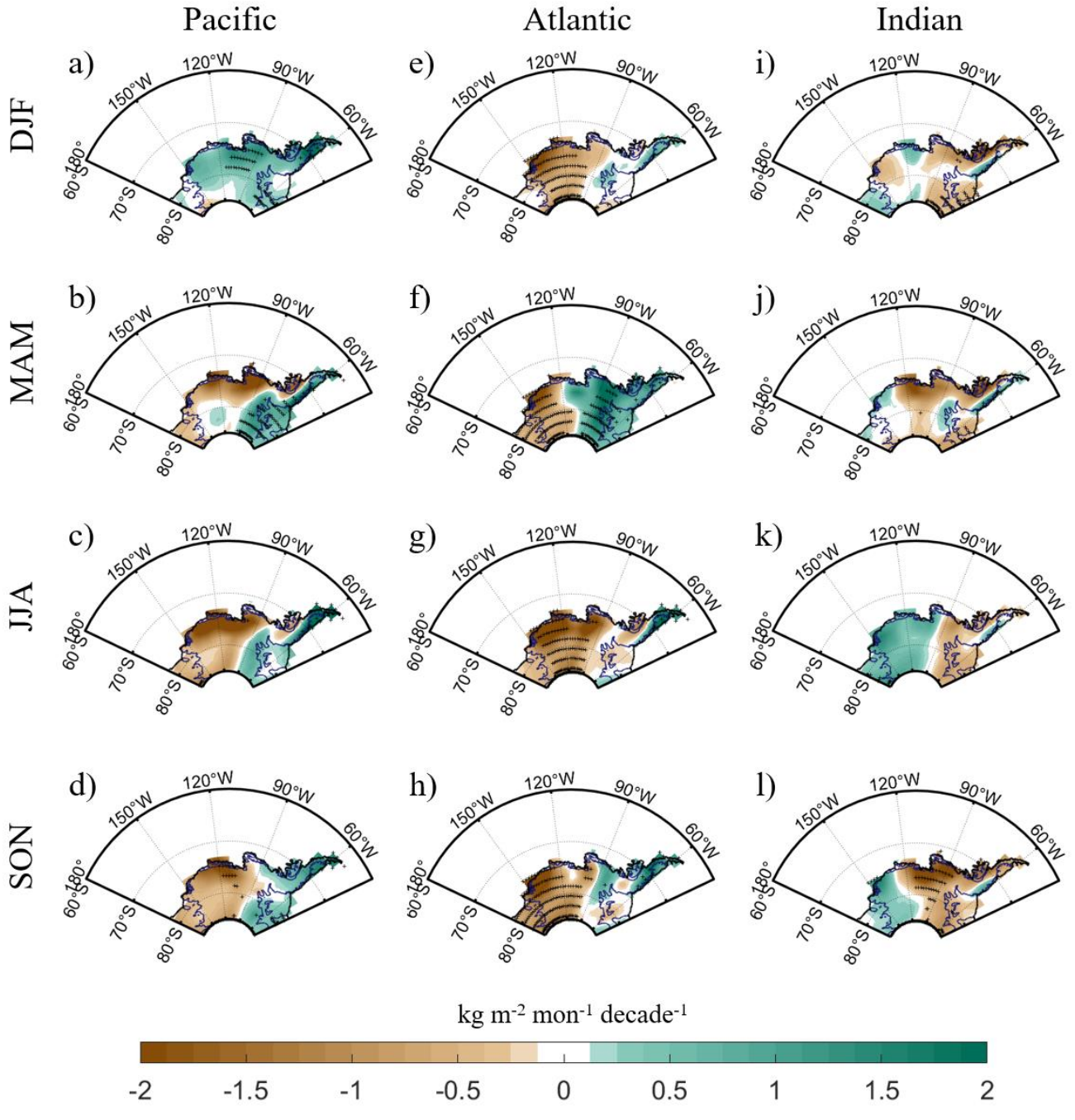

Figure 11 | Simulated response of precipitation trends to observed SST in three ocean basins. a-d show the response to Pacific SST in austral summer (**a**, December to February, DJF), autumn (**b**, March to May, MAM), winter (**c**, June to August, JJA) and spring (**d**, September to November, SON). **e-h** show the response to Atlantic SST. **i-l** show the response to Indian Ocean SST. Details about the simulated data are provided in the methods section (Section 2.2.2).

https://doi.org/10.5194/egusphere-2025-1381
Preprint. Discussion started: 21 May 2025

4 Conclusions and Outlook

In this study, through a synthesis analysis of 21 ice core records and five reanalysis datasets, we reveal a dipole-like SMB trend pattern over West Antarctica in recent decades, corroborating and extending previous studies (Dalaiden et al., 2022; Medley and Thomas, 2019; Wang et al., 2017). Statistical analysis and model simulations have shed light on the influence of multi-decadal SST trends on the dipole-like SMB pattern. Specifically, the cooling in the eastern tropical Pacific and warming in the tropical Atlantic, corresponding to a negative phase of the IPO and a positive phase of the AMO, are critical drivers. Further atmospheric dynamics analysis reveals that the associated tropical Pacific cooling and tropical Atlantic warming trigger Rossby wave trains, propagating to the West Antarctic and leading to low-pressure anomalies around the Amundsen and Bellingshausen Seas during the austral spring (SON) and autumn (MAM). These atmospheric circulation anomalies modulate the moisture transport from the Southern Ocean to the West Antarctic Ice Sheet, resulting in the contrasting precipitation pattern between its western and eastern parts.

This study reveals the influence of tropical decadal SST changes on Antarctic SMB, extending beyond the interannual relationships established in previous studies (Clem and Fogt, 2013; Lenaerts et al., 2019; Turner, 2004; Yuan et al., 2018). More importantly, our findings have substantial implications for future projections of the Antarctic Ice Sheet mass changes and consequent global sea level changes. As global warming continues, it is anticipated that the dynamic mass loss may accelerate. Concurrently, an anticipated increase in total SMB, due to an increase in atmospheric moisture-holding capacity, may partially compensate for the potential global sea level rise. However, our results suggest a potential influence of tropical SST changes on the future regional SMB changes in the context of global warming. Understanding the drivers and mechanisms of historical SMB trends is crucial for constraining the uncertainty in future projections of the Antarctic Ice Sheet mass loss and subsequent global sea level rise.

Throughout this paper, we single out the teleconnection patterns of the Pacific and Atlantic Oceans on the West Antarctic SMB, but the statistical analysis and the model simulation conducted do not well quantify the effect of each ocean basin. Moreover, the interactions between these two ocean basins and their joint effects on the West Antarctic SMB trends also require further investigation. Beyond West Antarctica, tropical-polar teleconnections are reported to affect broader areas, raising questions about how tropical oceans impact the SMB over the East Antarctic Ice Sheet. On the other hand, the relative importance of these teleconnections on the Antarctic SMB, in comparison to other factors including ozone depletion and greenhouse gas emissions remains poorly understood. Therefore, future investigations are urgently needed to isolate these effects and to evaluate their respective roles in shaping the Antarctic SMB.

Data and code availability

Met Office Hadley Centre sea ice and SST (HadISST) dataset is available at www.metoffice.gov.uk/hadobs/hadisst/. ERA5 reanalysis data are produced by the European Center for Medium-Range Weather Forecasts (ECWMF) and are accessible at https://www.ecmwf.int/en/forecasts/datasets/. JRA55 reanalysis data is provided by the Japan Meteorological Agency, which is available from http://search.diasjp.net/en/dataset/JRA55. CFSR reanalysis data is obtained from the National Climatic

https://doi.org/10.5194/egusphere-2025-1381
Preprint. Discussion started: 21 May 2025

Data Center (NCDC) and NCAR at https://rda.ucar.edu/datasets/ds093.2/. MERRA2 are provided by NASA's Global Modeling and Assimilation Office at https://disc.gsfc.nasa.gov/. NCEP2 reanalysis data is provided by the NCEP and NCAR at https://psl.noaa.gov/data/gridded/data.ncep.reanalysis2.html. Further data analysis and figures are made with Matlab version R2018a (MathWorks Inc., 2020), accessible at https://in.mathworks.com/products/matlab.html.

Author contributions

K.M., X.L., and J.L. conceptualized the study. K.M. and X.L. conducted the investigation and created the figures, while L.G. provided the ice core snow accumulation data. The model experiments were executed by X.L. and Y.H. K.M. prepared the initial draft of the manuscript, which was subsequently reviewed and edited by X.C., J.L., L.G., N.Y., Y.H., Y.W., and Y.M. All authors contributed to the final version of the manuscript.

Financial support

K.M. and X.L. were supported by the National Science Fund for Distinguished Young Scholars (42325605) and the National Natural Science Foundation of China (42176243).

Competing interests

The authors have the following competing interests: Some authors are members of the editorial board of journal The Cryosphere.

References

Agosta, C., Amory, C., Kittel, C., Orsi, A., Favier, V., Gallee, H., van den Broeke, M., Lenaerts, J., van Wessem, J., van de Berg, W., and Fettweis, X.: Estimation of the Antarctic surface mass balance using the regional climate model MAR (1979-2015) and identification of dominant processes, Cryosphere, 13, 281–296, https://doi.org/10.5194/tc-13-281-2019, 2019.

Bodart, J. A. and Bingham, R. J.: The Impact of the Extreme 2015–2016 El Niño on the Mass Balance of the Antarctic Ice Sheet, Geophys. Res. Lett., 46, 13862–13871, https://doi.org/10.1029/2019GL084466, 2019.

Bouchet, M., Landais, A., Grisart, A., Parrenin, F., Prié, F., Jacob, R., Fourré, E., Capron, E., Raynaud, D., Lipenkov, V. Y., Loutre, M.-F., Extier, T., Svensson, A., Legrain, E., Martinerie, P., Leuenberger, M., Jiang, W., Ritterbusch, F., Lu, Z.-T., and Yang, G.-M.: The Antarctic Ice Core Chronology 2023 (AICC2023) chronological framework and associated timescale for the European Project for Ice Coring in Antarctica (EPICA) Dome C ice core, Clim. Past, 19, 2257–2286, https://doi.org/10.5194/cp-19-2257-2023, 2023.

Bretherton, C. S., Widmann, M., Dymnikov, V. P., Wallace, J. M., and Bladé, I.: The Effective Number of Spatial Degrees of Freedom of a Time-Varying Field, J. Clim., 12, 1990–2009, https://doi.org/10.1175/1520-0442(1999)012<1990:TENOSD>2.0.CO;2, 1999.

Bromwich, D. H.: Snowfall in high southern latitudes, Rev. Geophys., 26, 149–168, https://doi.org/10.1029/RG026i001p00149, 1988.

https://doi.org/10.5194/egusphere-2025-1381
Preprint. Discussion started: 21 May 2025

Cavitte, M. G. P., Dalaiden, Q., Goosse, H., Lenaerts, J. T. M., and Thomas, E. R.: Reconciling the surface temperature-surface mass balance relationship in models and ice cores in Antarctica over the last 2 centuries, Cryosphere, 14, 4083–4102, https://doi.org/10.5194/tc-14-4083-2020, 2020.

Chemke, R., Previdi, M., England, M. R., and Polvani, L. M.: Distinguishing the impacts of ozone and ozone-depleting substances on the recent increase in Antarctic surface mass balance, Cryosphere, 14, 4135–4144, https://doi.org/10.5194/tc-14-4135-2020, 2020.

Clem, K. and Fogt, R.: South Pacific circulation changes and their connection to the tropics and regional Antarctic warming in austral spring, 1979-2012, J. Geophys. Res.: Atmos., 120, 2773–2792, https://doi.org/10.1002/2014JD022940, 2015.

Clem, K. R. and Fogt, R. L.: Varying roles of ENSO and SAM on the Antarctic Peninsula climate in austral spring, J. Geophys. Res. Atmos., 118, 11,481-11,492, https://doi.org/10.1002/jgrd.50860, 2013.

Clem, K. R., Renwick, J. A., McGregor, J., and Fogt, R. L.: The relative influence of ENSO and SAM on Antarctic Peninsula climate, J. Geophys. Res. Atmos., 121, 9324–9341, https://doi.org/10.1002/2016JD025305, 2016.

Dalaiden, Q., Schurer, A. P., Kirchmeier-Young, M. C., Goosse, H., and Hegerl, G. C.: West Antarctic Surface Climate Changes Since the Mid-20th Century Driven by Anthropogenic Forcing, Geophys. Res. Lett., 49, e2022GL099543, https://doi.org/10.1029/2022GL099543, 2022.

Ding, Q. and Steig, E. J.: Temperature Change on the Antarctic Peninsula Linked to the Tropical Pacific*, J. Climate, 26, 7570–7585, https://doi.org/10.1175/JCLI-D-12-00729.1, 2013.

Donat-Magnin, M., Jourdain, N. C., Gallée, H., Amory, C., Kittel, C., Fettweis, X., Wille, J. D., Favier, V., Drira, A., and Agosta, C.: Interannual variability of summer surface mass balance and surface melting in the Amundsen sector, West Antarctica, Cryosphere, 14, 229–249, https://doi.org/10.5194/tc-14-229-2020, 2020.

Ekaykin, A. A., Lipenkov, V. Ya., Kuzmina, I. N., Petit, J. R., MASSON-Delmotte, V., and Johnsen, S. J.: The changes in isotope composition and accumulation of snow at Vostok station, East Antarctica, over the past 200 years, Ann. Glaciol., 39, 569–575, https://doi.org/10.3189/172756404781814348, 2004.

Fogt, R. L. and Marshall, G. J.: The Southern Annular Mode: Variability, trends, and climate impacts across the Southern Hemisphere, WIREs Clim. Change, 11, e652, https://doi.org/10.1002/wcc.652, 2020.

Fox-Kemper, B., Hewitt, H. T., Xiao, C., Aðalgeirsdóttir, G., Drijfhout, S. S., Edwards, T. L., Golledge, N. R., Hemer, M., Kopp, R. E., Krinner, G., Mix, A., Notz, D., Nowicki, S., Nurhati, I. S., Ruiz, L., Sallée, J.-B., Slangen, A. B. A., and Yu, Y.: Ocean, Cryosphere and Sea Level Change, in: Climate Change 2021: The Physical Science Basis. Contribution of Working Group I to the Sixth Assessment Report of the Intergovernmental Panel on Climate Change, edited by: Masson-Delmotte, V., Zhai, P., Pirani, A., Connors, S. L., Péan, C., Berger, S., Caud, N., Chen, Y., Goldfarb, L., Gomis, M. I., Huang, M., Leitzell, K., Lonnoy, E., Matthews, J. B. R., Maycock, T. K., Waterfield, T., Yelekçi, O., Yu, R., and Zhou, B., Cambridge University Press, Cambridge, United Kingdom and New York, NY, USA, 1211–1362, https://doi.org/10.1017/9781009157896.011, 2021.

Frieler, K., Clark, P. U., He, F., Buizert, C., Reese, R., Ligtenberg, S. R. M., van den Broeke, M. R., Winkelmann, R., and Levermann, A.: Consistent evidence of increasing Antarctic accumulation with warming, Nat. Clim. Change, 5, 348–352, https://doi.org/10.1038/nclimate2574, 2015.

Gelaro, R., McCarty, W., Suárez, M. J., Todling, R., Molod, A., Takacs, L., Randles, C. A., Darmenov, A., Bosilovich, M. G., Reichle, R., Wargan, K., Coy, L., Cullather, R., Draper, C., Akella, S., Buchard, V., Conaty, A., Silva, A. M. da, Gu, W.,

https://doi.org/10.5194/egusphere-2025-1381
Preprint. Discussion started: 21 May 2025

Kim, G.-K., Koster, R., Lucchesi, R., Merkova, D., Nielsen, J. E., Partyka, G., Pawson, S., Putman, W., Rienecker, M., Schubert, S. D., Sienkiewicz, M., and Zhao, B.: The Modern-Era Retrospective Analysis for Research and Applications, Version 2 (MERRA-2), J. Climate, 30, 5419–5454, https://doi.org/10.1175/JCLI-D-16-0758.1, 2017.

Gocic, M. and Trajkovic, S.: Analysis of changes in meteorological variables using Mann-Kendall and Sen's slope estimator statistical tests in Serbia, Glob. Planet. Change, 100, 172–182, https://doi.org/10.1016/j.gloplacha.2012.10.014, 2013.

Henley, B. J., Gergis, J., Karoly, D. J., Power, S., Kennedy, J., and Folland, C. K.: A Tripole Index for the Interdecadal Pacific Oscillation, Clim. Dyn., 45, 3077–3090, https://doi.org/10.1007/s00382-015-2525-1, 2015.

Hersbach, H., Bell, B., Berrisford, P., Hirahara, S., Horányi, A., Muñoz-Sabater, J., Nicolas, J., Peubey, C., Radu, R., Schepers, D., Simmons, A., Soci, C., Abdalla, S., Abellan, X., Balsamo, G., Bechtold, P., Biavati, G., Bidlot, J., Bonavita, M., De Chiara, G., Dahlgren, P., Dee, D., Diamantakis, M., Dragani, R., Flemming, J., Forbes, R., Fuentes, M., Geer, A., Haimberger, L., Healy, S., Hogan, R. J., Hólm, E., Janisková, M., Keeley, S., Laloyaux, P., Lopez, P., Lupu, C., Radnoti, G., de Rosnay, P., Rozum, I., Vamborg, F., Villaume, S., and Thépaut, J.-N.: The ERA5 global reanalysis, Q. J. R. Meteorol. Soc., 146, 1999–2049, https://doi.org/10.1002/qj.3803, 2020.

Holland, D. M., Nicholls, K. W., and Basinski, A.: The Southern Ocean and its interaction with the Antarctic Ice Sheet, Science, 367, 1326–1330, https://doi.org/10.1126/science.aaz5491, 2020.

Jenkins, A., Shoosmith, D., Dutrieux, P., Jacobs, S., Kim, T. W., Lee, S. H., Ha, H. K., and Stammerjohn, S.: West Antarctic Ice Sheet retreat in the Amundsen Sea driven by decadal oceanic variability, Nat. Geosci., 11, 733–738, https://doi.org/10.1038/s41561-018-0207-4, 2018.

Jiang, J. and Zhou, T.: Agricultural drought over water-scarce Central Asia aggravated by internal climate variability, Nat. Geosci., 16, 154-+, https://doi.org/10.1038/s41561-022-01111-0, 2023.

Kanamitsu, M., Ebisuzaki, W., Woollen, J., Yang, S.-K., Hnilo, J. J., Fiorino, M., and Potter, G. L.: NCEP–DOE AMIP-II Reanalysis (R-2), Bulletin of the American Meteorological Society, 83, 1631–1644, https://doi.org/10.1175/BAMS-83-11-1631, 2002.

King, M. A. and Watson, C. S.: Antarctic Surface Mass Balance: Natural Variability, Noise, and Detecting New Trends, Geophys. Res. Lett., 47, e2020GL087493, https://doi.org/10.1029/2020GL087493, 2020.

Kittel, C., Amory, C., Agosta, C., Delhasse, A., Doutreloup, S., Huot, P.-V., Wyard, C., Fichefet, T., and Fettweis, X.: Sensitivity of the current Antarctic surface mass balance to sea surface conditions using MAR, Cryosphere, 12, 3827–3839, https://doi.org/10.5194/tc-12-3827-2018, 2018.

Kobayashi, S., Ota, Y., Harada, Y., Ebita, A., Moriya, M., Onoda, H., Onogi, K., Kamahori, H., Kobayashi, C., Endo, H., Miyaoka, K., and Takahashi, K.: The JRA-55 Reanalysis: General Specifications and Basic Characteristics, J. Meteorol. Soc. Jpn., II, 93, 5–48, https://doi.org/10.2151/jmsj.2015-001, 2015.

Lenaerts, J. T. M., Fyke, J., and Medley, B.: The Signature of Ozone Depletion in Recent Antarctic Precipitation Change: A Study With the Community Earth System Model, Geophys. Res. Lett., 45, 12,931-12,939, https://doi.org/10.1029/2018GL078608, 2018.

Lenaerts, J. T. M., Medley, B., van den Broeke, M. R., and Wouters, B.: Observing and Modeling Ice Sheet Surface Mass Balance, Rev. Geophys., 57, 376–420, https://doi.org/10.1029/2018RG000622, 2019.

https://doi.org/10.5194/egusphere-2025-1381
Preprint. Discussion started: 21 May 2025

Li, X., Gerber, E. P., Holland, D. M., and Yoo, C.: A Rossby Wave Bridge from the Tropical Atlantic to West Antarctica, J. Clim., 28, 2256–2273, https://doi.org/10.1175/JCLI-D-14-00450.1, 2015.

Li, X., Cai, W., Meehl, G. A., Chen, D., Yuan, X., Raphael, M., Holland, D. M., Ding, Q., Fogt, R. L., Markle, B. R., Wang, G., Bromwich, D. H., Turner, J., Xie, S.-P., Steig, E. J., Gille, S. T., Xiao, C., Wu, B., Lazzara, M. A., Chen, X., Stammerjohn, S., Holland, P. R., Holland, M. M., Cheng, X., Price, S. F., Wang, Z., Bitz, C. M., Shi, J., Gerber, E. P., Liang, X., Goosse, H., Yoo, C., Ding, M., Geng, L., Xin, M., Li, C., Dou, T., Liu, C., Sun, W., Wang, X., and Song, C.: Tropical teleconnection impacts on Antarctic climate changes, Nat. Rev. Earth Environ., 2, 680–698, https://doi.org/10.1038/s43017-021-00204-5, 2021.

Marshall, G. J., Thompson, D. W. J., and van den Broeke, M. R.: The Signature of Southern Hemisphere Atmospheric Circulation Patterns in Antarctic Precipitation, Geophys. Res. Lett., 44, 11,580-11,589, https://doi.org/10.1002/2017GL075998, 2017.

Medley, B. and Thomas, E. R.: Increased snowfall over the Antarctic Ice Sheet mitigated twentieth-century sea-level rise, Nat. Clim. Change, 9, 34–39, https://doi.org/10.1038/s41558-018-0356-x, 2019.

Medley, B., McConnell, J. R., Neumann, T. A., Reijmer, C. H., Chellman, N., Sigl, M., and Kipfstuhl, S.: Temperature and Snowfall in Western Queen Maud Land Increasing Faster Than Climate Model Projections, Geophys. Res. Lett., 45, 1472–1480, https://doi.org/10.1002/2017GL075992, 2018.

Meehl, G. A., Arblaster, J. M., Chung, C. T. Y., Holland, M. M., DuVivier, A., Thompson, L., Yang, D., and Bitz, C. M.: Sustained ocean changes contributed to sudden Antarctic sea ice retreat in late 2016, Nat. Commun., 10, 14, https://doi.org/10.1038/s41467-018-07865-9, 2019.

Nuncio, M. and Yuan, X.: The Influence of the Indian Ocean Dipole on Antarctic Sea Ice, J. Climate, 28, 2682–2690, https://doi.org/10.1175/JCLI-D-14-00390.1, 2015.

Oshima, K. and Yamazaki, K.: Difference in seasonal variation of net precipitation between the Arctic and Antarctic regions, Geophys. Res. Lett., 33, https://doi.org/10.1029/2006GL027389, 2006.

Pritchard, H. D., Ligtenberg, S. R. M., Fricker, H. A., Vaughan, D. G., van den Broeke, M. R., and Padman, L.: Antarctic ice-sheet loss driven by basal melting of ice shelves, Nature, 484, 502–505, https://doi.org/10.1038/nature10968, 2012.

Raphael, M. N., Marshall, G. J., Turner, J., Fogt, R. L., Schneider, D., Dixon, D. A., Hosking, J. S., Jones, J. M., and Hobbs, W. R.: The Amundsen Sea Low: Variability, Change, and Impact on Antarctic Climate, Bull. Am. Meteorol. Soc., 97, 111–121, https://doi.org/10.1175/BAMS-D-14-00018.1, 2016.

Rayner, N. A., Parker, D. E., Horton, E. B., Folland, C. K., Alexander, L. V., Rowell, D. P., Kent, E. C., and Kaplan, A.: Global analyses of sea surface temperature, sea ice, and night marine air temperature since the late nineteenth century, J. Geophys. Res.: Atmos., 108, https://doi.org/10.1029/2002JD002670, 2003.

Rignot, E., Mouginot, J., Scheuchl, B., van den Broeke, M., van Wessem, M. J., and Morlighem, M.: Four decades of Antarctic Ice Sheet mass balance from 1979–2017, Proc. Natl. Acad. Sci., 116, 1095–1103, https://doi.org/10.1073/pnas.1812883116, 2019.

Saha, S., Moorthi, S., Pan, H.-L., Wu, X., Wang, J., Nadiga, S., Tripp, P., Kistler, R., Woollen, J., Behringer, D., Liu, H., Stokes, D., Grumbine, R., Gayno, G., Wang, J., Hou, Y.-T., Chuang, H., Juang, H.-M. H., Sela, J., Iredell, M., Treadon, R., Kleist, D., Delst, P. V., Keyser, D., Derber, J., Ek, M., Meng, J., Wei, H., Yang, R., Lord, S., Dool, H. van den, Kumar, A., Wang, W., Long, C., Chelliah, M., Xue, Y., Huang, B., Schemm, J.-K., Ebisuzaki, W., Lin, R., Xie, P., Chen, M., Zhou, S.,

https://doi.org/10.5194/egusphere-2025-1381
Preprint. Discussion started: 21 May 2025

Higgins, W., Zou, C.-Z., Liu, Q., Chen, Y., Han, Y., Cucurull, L., Reynolds, R. W., Rutledge, G., and Goldberg, M.: The NCEP Climate Forecast System Reanalysis, Bull. Am. Meteorol. Soc., 91, 1015–1058, https://doi.org/10.1175/2010BAMS3001.1, 2010.

Saji, N. H., Goswami, B. N., Vinayachandran, P. N., and Yamagata, T.: A dipole mode in the tropical Indian Ocean, Nature, 401, 360–363, https://doi.org/10.1038/43854, 1999.

Schlesinger, M. E. and Ramankutty, N.: An oscillation in the global climate system of period 65–70 years, Nature, 367, 723–726, https://doi.org/10.1038/367723a0, 1994.

Shepherd, A., Ivins, E., Rignot, E., Smith, B., van den Broeke, M., Velicogna, I., Whitehouse, P., Briggs, K., Joughin, I., Krinner, G., Nowicki, S., Payne, T., Scambos, T., Schlegel, N., A, G., Agosta, C., Ahlstrøm, A., Babonis, G., Barletta, V., Blazquez, A., Bonin, J., Csatho, B., Cullather, R., Felikson, D., Fettweis, X., Forsberg, R., Gallee, H., Gardner, A., Gilbert, L., Groh, A., Gunter, B., Hanna, E., Harig, C., Helm, V., Horvath, A., Horwath, M., Khan, S., Kjeldsen, K. K., Konrad, H., Langen, P., Lecavalier, B., Loomis, B., Luthcke, S., McMillan, M., Melini, D., Mernild, S., Mohajerani, Y., Moore, P., Mouginot, J., Moyano, G., Muir, A., Nagler, T., Nield, G., Nilsson, J., Noel, B., Otosaka, I., Pattle, M. E., Peltier, W. R., Pie, N., Rietbroek, R., Rott, H., Sandberg-Sørensen, L., Sasgen, I., Save, H., Scheuchl, B., Schrama, E., Schröder, L., Seo, K.-W., Simonsen, S., Slater, T., Spada, G., Sutterley, T., Talpe, M., Tarasov, L., van de Berg, W. J., van der Wal, W., van Wessem, M., Vishwakarma, B. D., Wiese, D., Wouters, B., and The IMBIE team: Mass balance of the Antarctic Ice Sheet from 1992 to 2017, Nature, 558, 219–222, https://doi.org/10.1038/s41586-018-0179-y, 2018.

Thomas, E. R., Hosking, J. S., Tuckwell, R. R., Warren, R. A., and Ludlow, E. C.: Twentieth century increase in snowfall in coastal West Antarctica, Geophys. Res. Lett., 42, 9387–9393, https://doi.org/10.1002/2015GL065750, 2015.

Thomas, M., Ridley, J. K., Smith, I. J., Stevens, D. P., Holland, P. R., and Mackie, S.: Future Response of Antarctic Continental Shelf Temperatures to Ice Shelf Basal Melting and Calving, Geophys. Res. Lett., 50, e2022GL102101, https://doi.org/10.1029/2022GL102101, 2023.

Turner, J.: The El Nino-southern oscillation and Antarctica, Int. J. Climatol., 24, 1–31, https://doi.org/10.1002/joc.965, 2004.

Turner, J., Phillips, T., Thamban, M., Rahaman, W., Marshall, G. J., Wille, J. D., Favier, V., Winton, V. H. L., Thomas, E., Wang, Z., van den Broeke, M., Hosking, J. S., and Lachlan-Cope, T.: The Dominant Role of Extreme Precipitation Events in Antarctic Snowfall Variability, Geophys. Res. Lett., 46, 3502–3511, https://doi.org/10.1029/2018GL081517, 2019.

Wang, Y. and Xiao, C.: An Increase in the Antarctic Surface Mass Balance during the Past Three Centuries, Dampening Global Sea Level Rise, J. Climate, 36, 8127–8138, https://doi.org/10.1175/JCLI-D-22-0747.1, 2023.

Wang, Y., Ding, M., van Wessem, J. M., Schlosser, E., Altnau, S., van den Broeke, M. R., Lenaerts, J. T. M., Thomas, E. R., Isaksson, E., Wang, J., and Sun, W.: A Comparison of Antarctic Ice Sheet Surface Mass Balance from Atmospheric Climate Models and In Situ Observations, J. Climate, 29, 5317–5337, https://doi.org/10.1175/JCLI-D-15-0642.1, 2016.

Wang, Y., Thomas, E. R., Hou, S., Huai, B., Wu, S., Sun, W., Qi, S., Ding, M., and Zhang, Y.: Snow Accumulation Variability Over the West Antarctic Ice Sheet Since 1900: A Comparison of Ice Core Records With ERA-20C Reanalysis, Geophys. Res. Lett., 44, 11,482-11,490, https://doi.org/10.1002/2017GL075135, 2017.

van Wessem, J. M., van de Berg, W. J., Noël, B. P. Y., van Meijgaard, E., Amory, C., Birnbaum, G., Jakobs, C. L., Krüger, K., Lenaerts, J. T. M., Lhermitte, S., Ligtenberg, S. R. M., Medley, B., Reijmer, C. H., van Tricht, K., Trusel, L. D., van Ulft, L. H., Wouters, B., Wuite, J., and van den Broeke, M. R.: Modelling the climate and surface mass balance of polar ice sheets using RACMO2 – Part 2: Antarctica (1979–2016), Cryosphere, 12, 1479–1498, https://doi.org/10.5194/tc-12-1479-2018, 2018.

https://doi.org/10.5194/egusphere-2025-1381
Preprint. Discussion started: 21 May 2025

Xie, S.-P., Hu, K., Hafner, J., Tokinaga, H., Du, Y., Huang, G., and Sampe, T.: Indian Ocean Capacitor Effect on Indo–Western Pacific Climate during the Summer following El Niño, J. Climate, 22, 730–747, https://doi.org/10.1175/2008JCLI2544.1, 2009.

Yang, Y.-M., An, S.-I., Wang, B., and Park, J. H.: A global-scale multidecadal variability driven by Atlantic multidecadal oscillation, Natl. Sci. Rev., 7, 1190–1197, https://doi.org/10.1093/nsr/nwz216, 2020.

Yuan, X. and Martinson, D. G.: The Antarctic dipole and its predictability, Geophys. Res. Lett., 28, 3609–3612, https://doi.org/10.1029/2001GL012969, 2001.

Yuan, X., Kaplan, M. R., and Cane, M. A.: The Interconnected Global Climate System—A Review of Tropical–Polar Teleconnections, J. Climate, 31, 5765–5792, https://doi.org/10.1175/JCLI-D-16-0637.1, 2018.

Zhang, Y., Wallace, J. M., and Battisti, D. S.: ENSO-like Interdecadal Variability: 1900–93, J. Climate, 10, 1004–1020, https://doi.org/10.1175/1520-0442(1997)010<1004:ELIV>2.0.CO;2, 1997.